Murine Retinal Citrullination Declines With Age and is Mainly Dependent on Peptidyl Arginine Deiminase 4 (PAD4)

T. J. Hollingsworth,[1] Marko Z. Radic,[2] Sarka Beranova-Giorgianni,[3] Francesco Giorgianni,[3] Yanming Wang,[4] and Alessandro Iannaccone[5]

[1]Neuroscience Institute, University of Tennessee Health Science Center, Memphis, Tennessee, United States
[2]Department of Microbiology, Biochemistry and Immunology, University of Tennessee Health Science Center, Memphis, Tennessee, United States
[3]Department of Pharmaceutical Sciences, University of Tennessee Health Science Center, Memphis, Tennessee, United States
[4]Department of Biochemistry and Molecular Biology, Pennsylvania State University, University Park, Pennsylvania, United States
[5]Duke University School of Medicine, Duke Eye Center, Department of Ophthalmology, Durham, North Carolina, United States

Correspondence: Alessandro Iannaccone, Department of Ophthalmology, Duke University School of Medicine, Duke Eye Center, 2351 Erwin Road, DUMC Box 3802, Durham, NC 27710, USA; ai62@duke.edu.

Submitted: February 24, 2018
Accepted: July 7, 2018

Citation: Hollingsworth TJ, Radic MZ, Beranova-Giorgianni S, Giorgianni F, Wang Y, Iannaccone A. Murine retinal citrullination declines with age and is mainly dependent on peptidyl arginine deiminase 4 (PAD4). *Invest Ophthalmol Vis Sci*. 2018;59:3808–3815. https://doi.org/10.1167/iovs.18-24118

Purpose. Citrullination is a post-translational modification (PTM) that serves many normal physiological functions. Studies have shown that this PTM—along with expression of the catalyzing enzymes, peptidyl arginine deiminases (PADs)—are increased in autoimmune and age-related pathologies. PAD2 retinal expression has been previously documented in rat and human. Herein, we report on the expression levels and patterns of PAD2, PAD4, and retinal citrullination in the murine retina with age.

Methods. Wild-type (WT) and *Pad4*$^{-/-}$ (PAD4KO) mice ages 0.5, 0.75, 1, 3, 6, and 9 months were investigated after euthanasia and eye enucleation. Retinal lysates from 3-month-old mice were probed for PAD4 by western blot. Whole eyes were fixed, cryosectioned, and probed using an anti-PAD2/4 antibody (Ab), a specific anti-PAD4 Ab, and F95 anti-citrullinated peptide Ab. Fluorescent intensities were quantified with ImageJ.

Results. WT retinas show different levels of PAD4 expression in distinct retinal layers, with the most intense labeling in inner retinal layers, while PAD4KO mice lacked retinal PAD4. Using a nonspecific anti-PAD2/4 Ab, PAD reactivity observed in PAD4KO mice was attributed to PAD2. In WT, both PAD2 and PAD4 expression levels decrease significantly with age while low-level residual PAD2 expression was seen in PAD4KO mice. Citrullination levels in WT retinas paralleled PAD4 expression, with PAD4KO mice exhibiting consistently minimal citrullination.

Conclusions. Both PAD2 and PAD4 expression and citrullination decrease with age in the murine retina. However, in the absence of PAD4, retinal citrullination is nearly abolished, indicating that PAD4 is a main effector for retinal citrullination under physiological conditions.

Keywords: peptidyl arginine deiminase, post-translational modification, citrullination, retina, protein expression

Peptidyl arginine deiminases (PADs) are a family of enzymes responsible for the post-translational modification (PTM) of arginine residues to citrulline residues. The deiminating reaction catalyzed by PADs (also termed "citrullination") is a Ca^{2+}-dependent hydrolysis of the primary ketimine in arginine to a ketone by releasing a molecule of ammonia, forming citrulline, and conferring higher levels of protein hydrophobicity at the PTM site, resulting in changes in protein structure, function, and activity.[1]

There are five different PAD enzyme family members, PAD1 through 4 and PAD6. PADs and protein citrullination are known to be involved in multiple physiological and pathological systemic processes, such as epigenetics, inflammation, autoimmune disorders such as rheumatoid arthritis (RA) and multiple sclerosis (MS), Alzheimer's disease (AD), and cancer.[2–7] It has been reported that PAD2 is the main PAD in both retina and brain.[8–10] Previous work studying retinal PAD2 expression in rat models reported PAD2 expression and citrullination under physiological conditions, as well as a decline in both PAD2 and citrullination levels with age.[9] A number of proteins expressed in the retina and the brain undergo physiological citrullination, such as glial fibrillary acid protein (GFAP), myelin basic protein, myelin-associated glycoprotein, vimentin, and phosphodiesterases.[11] Using mass spectrometry-based proteomics approaches, other citrullinated proteins in the eye have been identified and implicated in glaucoma pathogenesis.[12] In addition, elevated citrullination levels, but not PAD2 levels, have been reported in post-mortem human eyes with age-related macular degeneration (AMD).[10]

Stimulated by these previous studies and by our growing interest in the role of inflammatory and immune-mediated events in retinal degenerative diseases,[13,14] we sought to

investigate the expression of PAD4 in retinal tissue. We recently reported, for the first time, expression and localization patterns of PAD4 in the mouse retina (Hollingsworth TJ, et al. *IOVS* 2015;56:ARVO E-Abstract 4636). To test the hypothesis that both PAD2 and PAD4 expression and citrullination experience age-related changes, we used western blots and fluorescent immunohistochemistry (IHC) on retinas from WT and PAD4KO mice, we quantified PAD2 and PAD4 expression levels and citrullination at specific early (0.5, 0.75, and 1 month) and later (3, 6, and 9 month) time points in mouse retinas. Our findings showed that both PAD2 and PAD4 are expressed in the retina, indicating that PAD4 appears to be the primary retinal PAD in the mouse retina under physiological conditions.

Methods

Animal Use

Animal care and use was in compliance with institutional guidelines and with the ARVO Statement for the Use of Animals in Ophthalmic and Vision Research. WT and PAD4KO mice,[15] both C57B/6J background, were aged to time points of 0.5, 0.75, 1, 3, 6, and 9 months. Mice were anesthetized by isoflurane and euthanized by cervical dislocation. Eyes were then enucleated and fixed for fluorescent IHC or retinas extracted for western blot analysis.

Primary Antibodies Used

To probe for PAD4 and retinal citrullination, rabbit anti-PAD4 (12373-1-AP; Proteintech Group, Inc., Rosemont, IL, USA) and mouse anti-citrullinated peptide clone F95 (MABN328; MilliporeSigma, Burlington, MA, USA) were used, respectively. Ascertaining PAD2 expression proved more challenging. We attempted to obtain the monoclonal antibody cited by Bonilha et al.,[10] but this was unavailable for our use. We then tried other commercially available antibodies, but none tested demonstrated sufficient, if any, binding of PAD2. To circumvent these challenges, a rabbit anti-PAD2/4 cross-reactive antibody was used to label for both PAD2 and PAD4 (12110-1-AP; Proteintech) in both WT and PAD4KO animals. Cross-reactivity was tested by western blot on purified recombinant PAD2-glutathione-S-transferase (rPAD2-GST) and purified rPAD4-GST fusion proteins (abcam, ab125591, and ab126910, respectively). Considering the absence of PAD4 in the KO mice (see "Results"), any residual PAD labeling in PAD4KO animals using this antibody was interpreted as attributable to PAD2, while labeling in WT animals was attributed to both PAD2 and PAD4 (total PAD labeling). Housekeeping protein GAPDH served as the loading control, and mouse anti-GAPDH (abcam, ab8245) antibodies were used for this purpose. Other antibodies used for IHC include rabbit anti-β-tubulin (abcam, a179513), mouse anti-glutamine synthetase (GS) (MAB302; MilliporeSigma), and chicken anti-neurofilament H (NFH) (PA1-10002; Thermo Fisher Scientific, Inc., Waltham, MA, USA).

Western Blotting

Two retinas each from WT and PAD4KO mice at 3 months of age were homogenized by sonication in 150 μL radioimmunoprecipitation assay buffer (10 mM Tris-HCl, pH 8.0, 1% Triton X-100, 0.1% sodium deoxycholate, 0.1% sodium dodecyl sulfate, 150 mM sodium chloride) with protease inhibitors (sc-24948; Santa Cruz Biotechnology, Inc., Santa Cruz, CA, USA) and centrifuged to pellet debris. We then used 20 ng of a purified PAD4-GST fusion protein (positive control for PAD4) and volumes equivalent to 10% of one retina (8 μL) from each lysate were loaded on a 15% SDS-PAGE gel, electrophoresed, and transferred to nitrocellulose overnight at 30 V at 4°C. The blot was then blocked in 3% bovine serum albumin (BSA) in phosphate buffered saline (PBS) with Tween-20 (PBST) for 1 hour at RT and subsequently probed for PAD4 using rabbit anti-PAD4 antibody and mouse anti-GAPDH overnight at 4°C. After washing in PBST, the blot was then probed using goat anti-rabbit IgG conjugated to IRDye800CW and goat anti-mouse IgG conjugated to IRDye650RD (LI-COR Biotechnology, Lincoln, NE, USA) for 1 hour at RT. After a final washing in PBST, the blot was imaged using the Odyssey system (LI-COR).

For a cross-reactivity test, 20 ng and 40 ng of each rPAD-GST fusion protein were loaded on a 15% SDS-PAGE gel, electrophoresed, and transferred to nitrocellulose overnight at 30 V at 4°C. The blot was then blocked in 3% BSA in PBST for 1 hour at RT and subsequently probed for PAD2 using rabbit anti-PAD4 antibody and for PAD4 using rabbit anti-PAD2/4 antibody overnight at 4°C. After washing in PBST, the blot was then probed using goat anti-rabbit IgG conjugated to IRDye 800CW for 1 hour at RT. After a final washing in PBST, the blot was imaged using the Odyssey system.

Fluorescent Immunohistochemistry

Whole eyes from 0.5 (14 days), 0.75 (21 days), 1-, 3-, 6-, and 9-month WT and PAD4KO mice were fixed in 4% paraformaldehyde in PBS, pH 7.4 overnight at 4°C, cryoprotected in 30% sucrose in PBS, pH 7.4, frozen in optimal cutting temperature (OCT) medium, and cryosectioned into 10 μm-thick sections. After washing away the OCT, sections were treated using heat-mediated antigen retrieval by boiling in 10mM sodium citrate, pH 6.0 with 0.05% Tween-20 for 1 hour. After cooling, slides were washed in PBS and subsequently blocked in 10% goat serum/5% BSA/0.5% Triton X-100 in PBS for 1 hour at RT. Following blocking, sections were incubated with one of the following primary antibody combinations in the same buffer overnight at 4°C: rabbit anti-PAD2/4 and mouse anti-citrullinated peptide clone F95; rabbit anti-PAD4 and mouse anti-citrullinated peptide clone F95; or rabbit anti-β-tubulin, mouse anti-GS, and chicken anti-NFH. After washing in PBS, slides were probed using either goat anti-rabbit IgG conjugated to AlexaFluor 488 (A-11034; Invitrogen, Carlsbad, CA, USA) and goat anti-mouse IgM conjugated to AlexaFluor 555 (A-24126; Invitrogen), or goat anti-rabbit IgG conjugated to AlexaFluor 488, goat anti-chicken IgY conjugated to AlexaFluor555 (A-21437; Invitrogen), goat anti-mouse IgG conjugated to AlexaFluor 647 (A-21236; Invitrogen), and DAPI (D-1306; Invitrogen). After washing in PBS, slides were mounted using Prolong Diamond Anti-Fade Mountant (P-36961; Invitrogen) and imaged using a Zeiss 710 Laser Scanning Confocal Microscope. All images were captured as Z-stacks and expressed as maximum intensity projections using the same laser power and gain settings to ensure comparability for intensity analysis. After background subtraction (obtained from no primary controls), fluorescent intensities were quantified using ImageJ and analyzed using the quotient of mean intensity and the area of the region-of-interest (neural retina/retinal pigment epithelium [RPE]).

Preplanned comparisons to investigate the effect of age on expression levels conducted by 1-way analysis of variance (ANOVA). An α-level of 0.05 was used to designate the level significance for these analyses. Post-hoc comparisons of average expression levels between individual time points and between genotypes were conducted by two-tailed *t*-tests. The Dunn-Sidák method was used to correct for multiple post-hoc comparisons made among the expression levels at each time

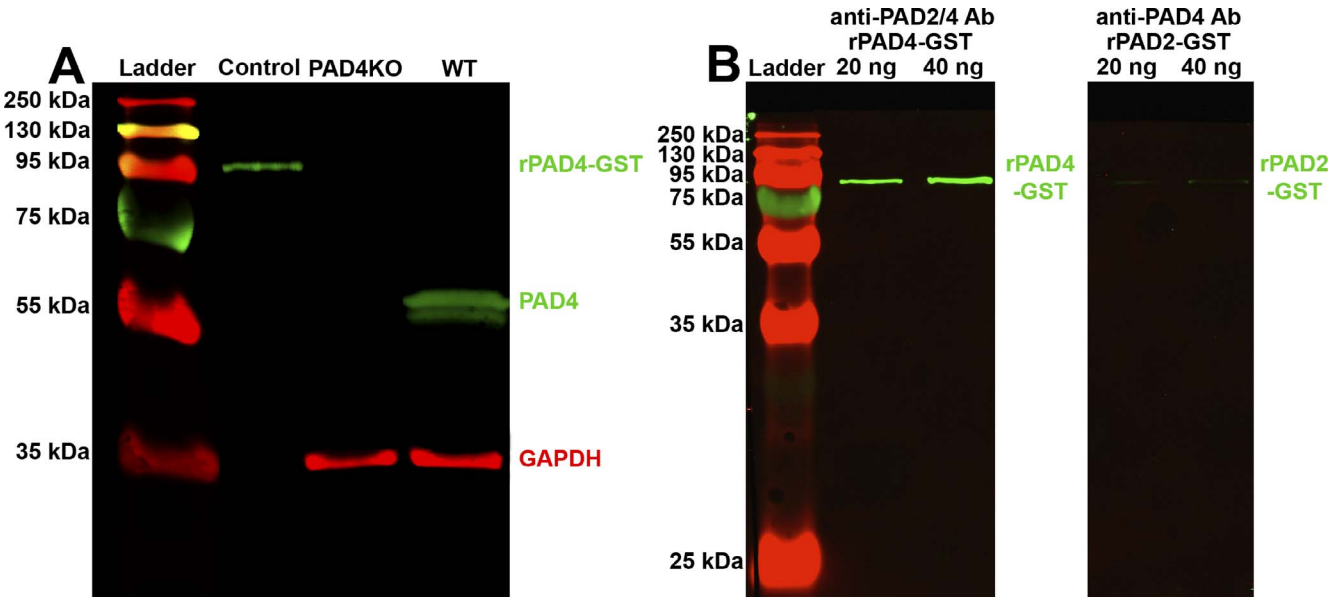

Figure 1. Western blot analysis of PAD4 expression in mouse retinal lysate and testing for antibody cross-reactivity. (**A**) Retinal lysates from WT and PAD4KO mice were electrophoresed and probed for PAD4 (*green*). GAPDH (*red*) served as a loading control. Control, 20 ng PAD4-GST fusion protein (*positive control*). At 3 months, WT mice exhibit a strong band at 65 kDa, indicative of PAD4, while PAD4KO animals exhibit no band, indicative of loss of PAD4. (**B**) 20 ng and 40 ng of rPAD4-GST (*lanes 2* and *3*) and rPAD2-GST (*lanes 4* and *5*) were electrophoresed and probed for PAD2 and PAD4 (*both green*), respectively. The anti-PAD2/4 antibody bound to PAD4 with a high affinity while the anti-PAD4 antibody bound negligibly to PAD2 protein.

point and between genotypes[16] (see Supplementary Tables S1–S3 for detailed analytical methods and summary statistics).

Results

Analysis of PAD4 Retinal Expression by Western Blot

To test the hypothesis that PAD4 is expressed in the murine retina, we performed western blotting on whole retinal lysates from WT and PAD4KO mice (Fig. 1A). In WT retina, a band was detected at approximately 65 kDa, the theoretical molecular weight of PAD4. In PAD4KO retina, no 65 kDa band was detected. A band at ~35 kDa was observed in both lanes, corresponding to the loading control GAPDH. The positive control of PAD4-GST fusion protein seen at ~95 kDa is consistent with the combined molecular weight of PAD4 (65 kDa) and GST (30 kDa).

Analysis of Ab Cross-Reactivity by Western Blot

To estimate the levels of cross-reactivity of the antibodies used, we performed western blotting on 20 ng and 40 ng of each protein (rPAD2-GST and rPAD4-GST) using the contrary antibody (i.e., rPAD2-GST was probed using anti-PAD4 and rPAD4-GST was probed using anti-PAD2/4; Fig. 1B). The non-specific anti-PAD2/4 antibody bound rPAD4-GST with similar affinity by densitometric analysis as anti-PAD4 antibody, while the anti-PAD4 antibody bound minimally to rPAD2-GST, consistent with specificity of the anti-PAD4 antibody for PAD4 and cross-reactivity between the non-specific anti-PAD2/4 antibody and PAD4 protein. Based on this outcome and on the assumption that no other PAD enzyme aside from PAD2 and PAD4 are expressed in the retina, the residual anti-PAD reactivity seen in PAD4KO mice by means of the non-specific anti-PAD2/4 antibody was interpreted as being attributable to PAD2.

Analysis of PAD4KO Retinal Morphology by Fluorescent IHC

The effect of PAD4KO on retinal morphology and histology has not been characterized to date. Thus, to address the possibility that PAD4KO retinas may differ intrinsically from WT retinas, sections from WT and PAD4KO mouse retinas were labeled for NFH (a marker for interneurons and ganglion cells), GS (a Müller cell marker), and β-tubulin (which labels the microtubular cytoskeletal components) and then compared (Supplementary Fig. S1). When compared with WT, PAD4KO retinal morphology appeared normal, with labeling patterns similar to WT retinas, suggesting that lack of PAD4 in the retina does not lead to overt anomalies in retinal architecture. We defer to in-depth investigations in future studies to determine whether unique changes in specific neuronal cell types or subtypes may be present in PAD4KO retinas that were not detected by this initial level of analysis.

Analysis of PAD4 Retinal Expression by Fluorescent IHC

By 1-way ANOVA, there was a significant change in overall PAD4 expression in WT retinas over time ($F = 8.953$, $P = 0.0007$; Supplementary Table S1). Quantitation of intensities by ImageJ analysis showed that by 0.75 month, PAD4 expression levels were already reduced by approximately 25% of the 0.5-month levels and that, after a transient smaller peak of expression around 1 month, PAD4 expression remained at approximately 20%–25% of the 0.5-month through 9-month levels (Fig. 2A). WT PAD4 localization patterns changed as well over time, shifting from the pan-retinal and punctate nuclear labeling, seen at early ages, to a transient peak of expression in the outer retina at 1 month, followed by a labeling pattern favoring inner retinal cells at 3 and 6 months (Fig. 2B). In PAD4KO retinas, minimal residual PAD4 labeling was observed under physiological conditions, further validating the western blot findings. Thus, no true time-dependent changes could be documented. As expected,

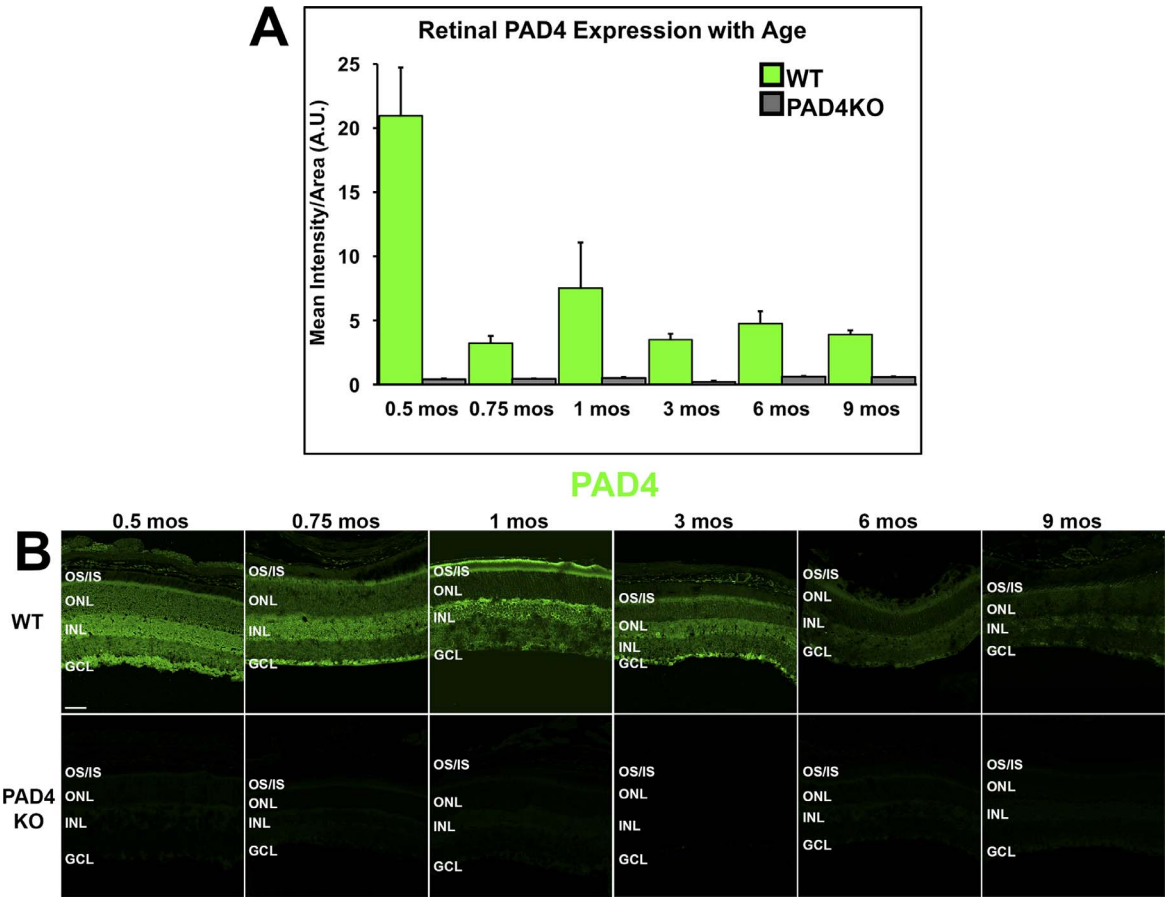

FIGURE 2. IHC analysis of PAD4 localization and expression levels in the mouse retina. (**A**) PAD4 expression levels were quantified using densitometric analysis of fluorescent intensities across the neural retina using ImageJ and plotted as mean intensity divided by area as a function of age. Data are expressed as the mean ± SEM (error bars, $n = 3$). A steep decline in immunoreactivity was seen in WT mice between 0.5 and 0.75 months (14 vs. 21 days) of age, with subsequent peaks at 1 month and between 3 and 6 months. (**B**) Immunolabeling of PAD4 (*green*) in WT and PAD4KO mouse retinas at serial time points. GCL, ganglion cell layer; INL, inner nuclear layer; ONL, outer nuclear layer; OS/IS, photoreceptor outer segments/inner segments. *Scale bar*: 50 μm.

differences in expression levels were significantly different between WT and PAD4KO animals. At higher magnification, PAD4 expression is strongest in inner retinal cells of the ganglion cell layer and the inner nuclear layer similarly to the patterns of citrullination (Supplementary Fig. S2).

Analysis of Total PAD and PAD2 Retinal Expression by Fluorescent IHC

To document the overall expression pattern of PADs in the retina, to compare PAD4 versus PAD2 expression levels in the retina and to address the question whether PAD2 expression declines with age in mice as has been shown in rats,[9] we performed fluorescent IHC experiments using the non-specific anti-PAD2/4 antibody in both WT mice and in the PAD4KO mice. In the latter, any residual immunoreactivity detected by this non-specific antibody was interpreted as attributable to PAD2 (Fig. 3A). Experiments were conducted on retinal sections at corresponding time points as in the previous experiments for direct comparison to PAD4 data.

Figure 3A illustrates the significant physiological reduction in total PAD immunoreactivity over time in WT mice ($F = 4.9318$, $P = 0.0072$; Supplementary Table S2). By 9 months, total PAD expression levels were approximately 30% that of 0.5-month levels. The decline was more gradual and steadier than for PAD4 alone, and no secondary transient peak at 1 month was observed. The top panels in Figure 3B illustrate the changes in immunoreactivity patterns observed with age for total PAD expression. As of age 0.75 month, little to no PAD reactivity was seen at the ONL level, and most of the immunoreactivity remained localized to the inner and outer plexiform layers of the retina.

Consistent with the existing evidence that PAD2 expression declines with age in the rat retina,[9] PAD2 residual immunoreactivity seen in the PAD4KO mice with the PAD2/4 non-specific Ab (Fig. 3A, gray bars) also decreased with age, although this effect was not nearly as pronounced as for PAD4 ($F = 4.3753$, $P = 0.0131$; Supplementary Table S2). Similar to PAD4, PAD2 residual immunoreactivity seen in the PAD4KO mice appeared localized initially across the entire retina (Fig. 3B), although it lacked the punctate nuclear staining observed in PAD4 labeling (Fig. 2B). However, unlike PAD4, after age 0.5 month, both PAD2 expression and localization remained almost unchanged in PAD4KO retinas, regardless of age (Fig. 3B). A comparison between total PAD reactivity and PAD2 residual reactivity suggests that the majority of the signal detected in the WT mice under physiological conditions is attributable to PAD4.

Analysis of Retinal Citrullination by Fluorescent IHC

Since PADs mediate citrullination of peptides and since we observed levels of expression of PADs that changed with age

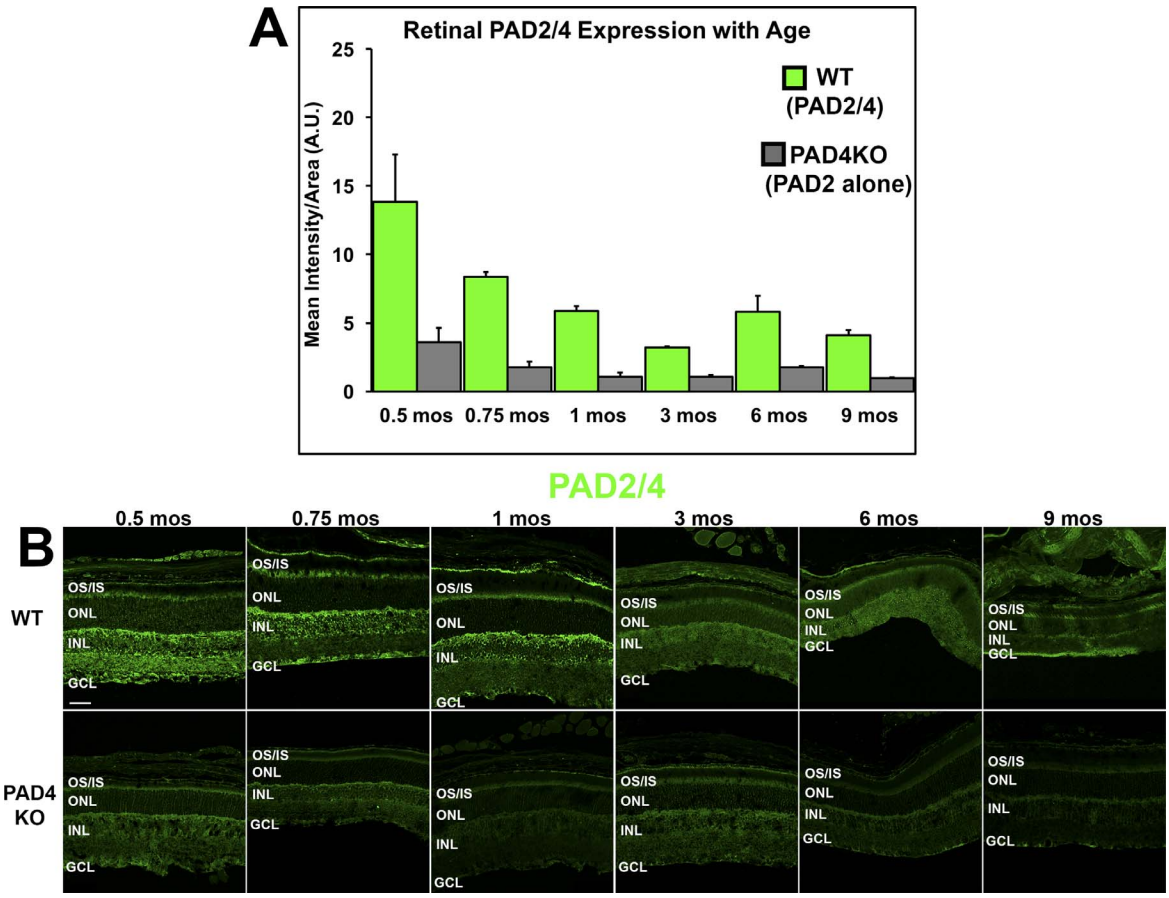

FIGURE 3. IHC localization and expression levels of total PAD (WT) and PAD2 (PAD4KO) in the mouse retina. (**A**) Expression levels of total PAD (WT) and residual PAD2 (PAD4KO) were quantified using densitometric analysis of fluorescent intensities across the neural retina using ImageJ and plotted as mean intensity divided by area as a function of age. Data are expressed as the mean ± SEM (error bars, $n = 3$). A decline in both total PAD immunoreactivity and residual PAD2 reactivity over time was seen in both WT mice and PAD4KO mice, respectively. (**B**) Immunolabeling (*in green*) attributable to both PAD2 and PAD4 (total PAD reactivity) in WT mice and residual PAD2 reactivity seen in PAD4KO mouse retinas at serial time points. GCL, ganglion cell layer; INL, inner nuclear layer; ONL, outer nuclear layer; OS/IS, photoreceptor outer segments/inner segments. *Scale bar*: 50 μm.

that suggest a preeminent PAD4 expression, we then examined the levels of retinal citrullination under physiological conditions over time using anti-citrullinated peptide clone F95 to test our hypothesis that retinal citrullination experiences age-dependent changes. Mouse retinal sections at time points corresponding to those previously shown in Figures 2 and 3 were also used for these experiments.

Similar to the expression levels of PAD4, under physiological conditions, younger animals exhibited markedly higher levels of citrullination than did older animals. Reactivity declined significantly over time as assessed by 1-way ANOVA ($F = 8.846$, $P = 0.0006$; Supplementary Table S3), reaching negligible levels by 9 months. A transient second peak of citrullinated peptides was seen around 3 months in WT mice. In the absence of PAD4, residual retinal citrullination under physiological conditions was nearly undetectable at all time points (Fig. 4A), supporting the conclusion that PAD4 is the primary retinal PAD.

Citrullination patterns in WT retinas were heavily nuclear in localization at early ages, changing to a prevailingly inner retinal pattern of expression at later ages as seen for PAD4 (Fig. 4B). Prior to the 3-month citrullination secondary peak, 1-month-old animals lost the heavy nuclear citrullination and, in fact, lacked significant citrullination compared with other ages. After the peak at 3 months, stronger expression at inner retinal level was observed, mirroring again closest the dynamics of PAD4 expression. To investigate further the subcellular location of citrullinated peptides, images at higher magnification were also obtained. Similar to PAD4 expression patterns, citrullination was strongest in inner retinal cells of the ganglion cell layer and the inner nuclear layer (Supplementary Fig. S2).

DISCUSSION

PAD-mediated citrullination (i.e., deimination) is a calcium-dependent PTM that is essential for the proper function of many cell types and homeostatic maintenance for an organism. Protein citrullination alters the electrochemical properties of the modified proteins, which in turn has important effects on the conformation, stability, and protein-protein interactions of those polypeptides. Some normal targets of PAD catalysis include histones, filaggrin, actin, keratin, GFAP, and vimentin. The citrullination of histones serves an epigenetic modulatory function in some cells, while in neutrophils it serves as the initiating step in the process of neutrophil extracellular trap (NET) formation, a specialized method of innate immunity in which neutrophil chromatin is ejected from the cell due to citrullination and ensnares pathogens.[17,18] In the retina, a number of additional citrullination targets have been identified by mass spectrometry, including various isoforms of the annexin, septin, and several members of the dihydropyrimidi-

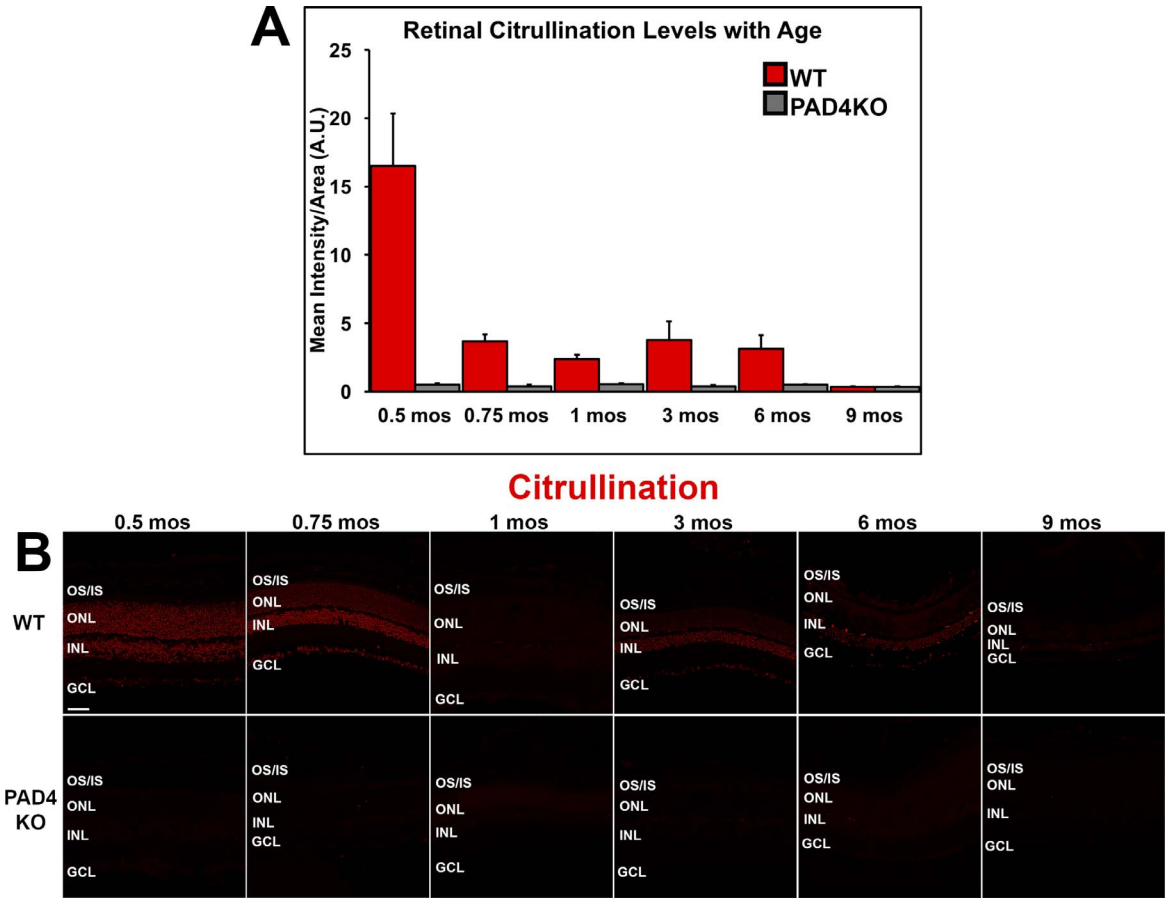

FIGURE 4. Immunohistochemical analysis of citrullinated peptide localization and levels in the mouse retina. (**A**) Citrullinated peptide expression levels were quantified using densitometric analysis of fluorescent intensities across the neural retina using ImageJ and plotted as mean intensity divided by area as a function of age. Data are expressed as the mean ± SEM (error bars, $n = 6$). Reactivity declined over time, reaching negligible levels by 9 months under physiological conditions. (**B**) Immunolabeling of citrullinated peptides (*red*) in WT and PAD4KO mouse retinas at increasing ages. The pattern of expression of citrullinated peptides over time mirrored closest the dynamics of PAD4 expression. GCL, ganglion cell layer; INL, inner nuclear layer; ONL, outer nuclear layer; OS/IS, photoreceptor outer segments/inner segments. *Scale bar*: 50 μm.

nase-related protein families: gamma enolase, lumican, mimecan, and various myelin-related proteins.[11] Citrullination of these and other target proteins plays a pivotal role in apotosis, cell differentiation, cytoskeletal changes, gene regulation, and inflammation.[2,7,19–21]

PAD2 has been reported to be the main neuronal PAD in the brain and the eye.[11] Citrullination has also been observed in microglial cells.[11] The patterns of physiological retinal citrullination as a function of aging were first investigated by Bhattacharya and associates in rat tissues at 3, 6, 18, and 24 months.[9,11] Their studies showed widespread retinal citrullination in multiple layers and demonstrated a physiological decline in retinal citrullination with age. Citrullination was also observed in microglial cells.[11] They also reported unpublished observations of elevated retinal citrullination in light-damaged rat and mouse studies.[11] Their study focused on PAD2 expression patterns, and no data on retinal PAD4 expression were reported. Citrullination and PAD2 protein expression were then investigated in human glaucoma and AMD tissues, found to be elevated in these conditions.[10,12] Taken together, these age-related disorders showed patterns of reactivity opposite to the age-related patterns physiologically seen in rodents, suggesting a role for citrullination in disease-related events. Interestingly, it was also shown that, while citrullination is elevated in macular tissues of AMD patients, PAD2 expression was not elevated.[10] These authors concluded that the process could be attributed to reduced turnover of citrullinated proteins in AMD tissues. However, PAD4 expression was not investigated.[10] Thus, it is also possible that, in parallel to the increased macular citrullinated peptide expression, elevated PAD4 expression may be present in AMD tissues.

Our study also confirmed the physiologically widespread presence of citrullinated proteins in the mouse retina across multiple retinal layers in a pattern consistent with that reported by Bhattacharya et al. in rats.[9,11] To gain further insight into the physiological expression patterns of PADs and their age-related changes, we chose to investigate young (0.5, 0.75, and 1 month) mice, contrasting them with older mice through 9 months. Consistent with the data by Bhattacharya et al.,[9,11] total PAD reactivity also declined with age in mouse tissues. We further demonstrated that there was a significant interaction between time and both PAD2 and PAD4 expression, as well as citrullination, except in the PAD4KO animals; this provided evidence that in the absence of PAD4, the vast majority of retinal citrullination is ablated.

In line with its expected nuclear localization, PAD4-specific reactivity was observed in our experiments primarily at the nuclear level in the mouse retinal tissue. The highly nuclear localization of citrullinated peptides observed in our experiments suggest an epigenetic modulatory function for retinal citrullination occurring in retinal neurons. However, we

observed a shift of citrullination from ONL, INL, and GCL nuclei to a smaller subset of retinal cells.

The near absence of retinal protein citrullination observed in the PAD4KO mouse suggests that PAD4 is the main mediator of physiological retinal citrullination. Considering this and the continued expression of PAD2 in the PAD4KO retina, it is possible that PAD2 could serve as a compensatory citrullination pathway under such conditions; however, to test this hypothesis, further studies are needed involving substrate specificities for the two enzymes and identification of possible targets for citrullination. Citrullination of arginine residues in glial proteins such as GFAP and vimentin occurs in both normal and diseased states. Thus, PADs likely serve a role in retinal homeostasis both under normal conditions and in pathological states, such as inflammation.[21,22] Consistent with this possibility, it has been reported very recently that both PAD2 and PAD4 are expressed in mouse retinas and that both citrullinated peptides and PAD4 (but not PAD2) were elevated in Müller glial cells shortly after acute alkali injury to the anterior segment.[22] In that study, the age of the mice used in the experiments was not specified, and both the patterns and the intensity of retinal reactivity differed significantly from those that we and Bhattacharya et al.[9,11] observed. Technical differences, including the utilization of different PAD antibodies, may explain these discrepancies. With these caveats in mind, this recent report indirectly corroborates our conclusion that PAD4 is likely to serve as the main retinal PAD, suggesting that PAD4 may have this preeminent role under both physiological and pathological conditions.

After the initial heightened levels of citrullination at 0.5 month (possibly due to an increase in reactive oxygen species formation due to eyelid opening and to physiologically high levels of apoptosis in retinal ganglion cells in the immediate postnatal period),[23,24] we observed in earlier ages a steep decline in PAD4 expression between 0.5 (i.e., 14 days) and 0.75 (i.e., 21 days) months of age, followed by a much slower rate of decline at subsequent time points. The pattern of decline in residual PAD2 reactivity seen in PAD4KO mice, however, was more gradual. This finding suggests that further studies of PAD activity, citrullination levels, and the targets of retinal PADs could lend important insight into the processes taking place during early postnatal retinal development.

Protein citrullination is known to trigger specific autoreactivities in RA.[25] Likewise, citrullinated proteins in the eye may also act locally as autoantigens.[26] For example, a known citrullinated retinal/RPE protein is annexin A5 (ANXA5).[11] This anti-apoptotic protein is an autophagy stimulator[27] involved in the modulation of the immune response.[28–30] ANXA5 is one of the autoantigens implicated in RA, as well as in other systemic autoimmune diseases such as the antiphospholipid syndrome and lupus.[28,30] Of specific relevance to AMD, ANXA5 is upregulated in neovascular AMD and is a documented component of drusen.[31,32] Anti-ANXA5 autoreactivity was also the single most statistically significant human macular tissue autoantigen that we recently identified in AMD.[13] Thus, extrapolating our findings to human pathophysiology, the increased retinal protein citrullination reported by Bonilha et al.[10] in human AMD tissues may play a role in AMD via an autoimmune-mediated mechanism, as in other systemic disorders.

In summary, both PAD2 and PAD4 are expressed in the mouse retina, and both experience a physiological age-related decline. PAD4 appears to be the main retinal PAD and, as such, the main effector of protein citrullination under normal conditions in the murine retina. Further investigations into the roles of PADs in the retina promise to lead to better understanding of retinal biology and development, as well as the pathogenesis of human retinal disease.

Acknowledgments

Supported by National Eye Institute/National Institutes of Health R01 EY022706 (AI, FG) and unrestricted grant to the Duke Eye Center from Research to Prevent Blindness, Inc., New York, New York, United States.

Disclosure: **T.J. Hollingsworth**, None; **M.Z. Radic**, None; **S. Beranova-Giorgianni**, None; **F. Giorgianni**, None; **Y. Wang**, None; **A. Iannaccone**, None

References

1. Vossenaar ER, Zendman AJ, van Venrooij WJ, Pruijn GJ. PAD, a growing family of citrullinating enzymes: genes, features and involvement in disease. *Bioessays*. 2003;25:1106–1118.
2. Witalison EE, Thompson PR, Hofseth LJ. Protein arginine deiminases and associated citrullination: physiological functions and diseases associated with dysregulation. *Curr Drug Targets*. 2015;16:700–710.
3. Acharya NK, Nagele EP, Han M, et al. Neuronal PAD4 expression and protein citrullination: possible role in production of autoantibodies associated with neurodegenerative disease. *J Autoimmun*. 2012;38:369–380.
4. Calabrese R, Zampieri M, Mechelli R, et al. Methylation-dependent PAD2 upregulation in multiple sclerosis peripheral blood. *Mult Scler*. 2012;18:299–304.
5. Moscarello MA, Mastronardi FG, Wood DD. The role of citrullinated proteins suggests a novel mechanism in the pathogenesis of multiple sclerosis. *Neurochem Res*. 2007;32:251–256.
6. Turunen S, Huhtakangas J, Nousiainen T, et al. Rheumatoid arthritis antigens homocitrulline and citrulline are generated by local myeloperoxidase and peptidyl arginine deiminases 2, 3 and 4 in rheumatoid nodule and synovial tissue. *Arthritis Res Ther*. 2016;18:239.
7. Wang Y, Wysocka J, Sayegh J, et al. Human PAD4 regulates histone arginine methylation levels via demethylimination. *Science*. 2004;306:279–283.
8. Bhattacharya SK, Bhat MB, Takahara H. Modulation of peptidyl arginine deiminase 2 and implication for neurodegeneration. *Curr Eye Res*. 2006;31:1063–1071.
9. Bhattacharya SK, Sinicrope B, Rayborn ME, Hollyfield JG, Bonilha VL. Age-related reduction in retinal deimination levels in the F344BN rat. *Aging Cell*. 2008;7:441–444.
10. Bonilha VL, Shadrach KG, Rayborn ME, et al. Retinal deimination and PAD2 levels in retinas from donors with age-related macular degeneration (AMD). *Exp Eye Res*. 2013;111:71–78.
11. Bhattacharya SK. Retinal deimination in aging and disease. *IUBMB Life*. 2009;61:504–509.
12. Bhattacharya SK, Crabb JS, Bonilha VL, Gu X, Takahara H, Crabb JW. Proteomics implicates peptidyl arginine deiminase 2 and optic nerve citrullination in glaucoma pathogenesis. *Invest Ophthalmol Vis Sci*. 2006;47:2508–2514.
13. Iannaccone A, Giorgianni F, New DD, et al. Circulating autoantibodies in age-related macular degeneration recognize human macular tissue antigens implicated in autophagy, immunomodulation, and protection from oxidative stress and apoptosis. *PLoS One*. 2015;10:e0145323.
14. Iannaccone A, Hollingsworth TJ, Koirala D, et al. Retinal pigment epithelium and microglia express the CD5 antigen-like protein, a novel autoantigen in age-related macular degeneration. *Exp Eye Res*. 2017;155:64–74.
15. Li P, Li M, Lindberg MR, Kennett MJ, Xiong N, Wang Y. PAD4 is essential for antibacterial innate immunity mediated by neutrophil extracellular traps. *J Exp Med*. 2010;207:1853–1862.

16. Sokal RR, Rohlf FJ. Single-classification analysis of variance. In: *Biometry: The Principles and Practice of Statistics in Biological Research*. 3rd ed. New York, NY: Freeman; 1995: 229–240.
17. Dwivedi N, Neeli I, Schall N, et al. Deimination of linker histones links neutrophil extracellular trap release with autoantibodies in systemic autoimmunity. *FASEB J*. 2014;28: 2840–2851.
18. Dwivedi N, Radic M. Citrullination of autoantigens implicates NETosis in the induction of autoimmunity. *Ann Rheum Dis*. 2014;73:483–491.
19. Christophorou MA, Castelo-Branco G, Halley-Stott RP, et al. Citrullination regulates pluripotency and histone H1 binding to chromatin. *Nature*. 2014;507:104–108.
20. Nakashima K, Arai S, Suzuki A, et al. PAD4 regulates proliferation of multipotent haematopoietic cells by controlling c-myc expression. *Nat Commun*. 2013;4:1836.
21. Neeli I, Khan SN, Radic M. Histone deimination as a response to inflammatory stimuli in neutrophils. *J Immunol*. 2008;180: 1895–1902.
22. Wizeman JW, Nicholas AP, Ishigami A, Mohan R. Citrullination of glial intermediate filaments is an early response in retinal injury. *Mol Vis*. 2016;22:1137–1155.
23. Liu L, Wu J, Zhou X, Chen Z, Zhou G. The impact of visible light on the immature retina: a model of early light exposure in neonatal mice. *Brain Res Bull*. 2012;87:534–539.
24. Dreher B, Potts RA, Bennett MR. Evidence that the early postnatal reduction in the number of rat retinal ganglion cells is due to a wave of ganglion cell death. *Neurosci Lett*. 1983; 36:255–260.
25. Diaz FJ, Rojas-Villarraga A, Salazar JC, Iglesias-Gamarra A, Mantilla RD, Anaya JM. Anti-CCP antibodies are associated with early age at onset in patients with rheumatoid arthritis. *Joint Bone Spine*. 2011;78:175–178.
26. Riedhammer C, Weissert R. Antigen presentation, autoantigens, and immune regulation in multiple sclerosis and other autoimmune diseases. *Front Immunol*. 2015;6:322.
27. Ghislat G, Aguado C, Knecht E. Annexin A5 stimulates autophagy and inhibits endocytosis. *J Cell Sci*. 2012;125:92–107.
28. Alessandri C, Conti F, Pendolino M, Mancini R, Valesini G. New autoantigens in the antiphospholipid syndrome. *Autoimmun Rev*. 2011;10:609–616.
29. Cederholm A, Frostegard J. Annexin A5 in cardiovascular disease and systemic lupus erythematosus. *Immunobiology*. 2005;210:761–768.
30. Iaccarino L, Ghirardello A, Canova M, et al. Anti-annexins autoantibodies: their role as biomarkers of autoimmune diseases. *Autoimmun Rev*. 2011;10:553–558.
31. Lederman M, Weiss A, Chowers I. Association of neovascular age-related macular degeneration with specific gene expression patterns in peripheral white blood cells. *Invest Ophthalmol Vis Sci*. 2010;51:53–58.
32. Rayborn ME, Sakaguchi H, Shadrach KG, Crabb JW, Hollyfield JG. Annexins in Bruch's membrane and drusen. *Adv Exp Med Biol*. 2006;572:75–78.

Investigative Ophthalmology & Visual Science